0026-895X/94/061149-07$03.00/0

MOLECULAR PHARMACOLOGY, 46:1149-1155, 1994.

Gating Properties of Mutant Acetylcholine Receptors

MARIA L. AYLWIN and MICHAEL M. WHITE

Department of Physiology, Medical College of Pennsylvania, Philadelphia, Pennsylvania 19129 (M.L.A., M.M.W.), and Department of Physiology, University of Pennsylvania School of Medicine, Philadelphia, Pennsylvania 19104 (M.L.A.)

Received June 13, 1994; Accepted September 20, 1994

SUMMARY

A number of affinity labeling studies have identified several tyrosine residues in the α subunit of the nicotinic acetylcholine receptor as being in or near the ligand binding site. Studies employing site-directed mutagenesis of these residues (αY93, αY190, and αY198; the notation used is subunit/amino acid/position in the *Torpedo* receptor/substitution) in mouse muscle, *Torpedo* electroplax, and α7 neuronal acetylcholine receptors have demonstrated that substitution of phenylalanine for tyrosine results in a shift towards higher concentrations in the macroscopic dose-response curves for acetylcholine-elicited currents from voltage-clamped *Xenopus* oocytes that express the receptors. This decrease in apparent affinity has been ascribed to either a reduction in binding affinity or a reduction in the coupling of agonist binding to ion channel opening; both mechanisms would give rise to shifts in the dose-response curves. We have used kinetic analysis of ion channel gating at the single-channel level to obtain estimates for the rate constants associated with the ligand binding and channel opening steps for wild-type, αY93F, and αY198F receptors. The results suggest that the underlying cause of the shifts in the macroscopic dose-response curves is a reduction in acetylcholine affinity for the resting activatable state of the receptor. Furthermore, it is the association rate for agonist binding, rather than the dissociation rate, that is most affected by the mutations.

The muscle-type nicotinic AChR is a transmembrane glycoprotein complex consisting of four subunits, in a stoichiometry of $\alpha_2\beta\gamma\delta$, that is involved in vertebrate neuromuscular transmission and the generation of high-voltage impulses by fish electric organs. The binding of two agonist molecules to the receptor induces a conformational change that results in the opening of a cation-selective ion channel. The receptor is a member of the ligand-gated ion channel gene superfamily, which includes neuronal nicotinic AChRs, glycine receptors, γ-aminobutyric acid type A receptors, and serotonin type 3 receptors (1, 2).

A number of elegant affinity labeling studies have localized portions of the agonist binding site to several domains of the α subunit, and mutagenesis studies have provided evidence for the role of several aromatic amino acid residues in both the muscle-type α and neuronal α7 subunits in channel gating, in particular αY93, αW149, αY190, and αY198 (the notation used is subunit/amino acid/position in the *Torpedo* subunit) (for recent reviews, see Refs. 3 and 4). In each of these cases, replacement of the indicated residue by phenylalanine led to a decrease in the apparent affinity for ACh, as measured by shifts in the midpoint of dose-response curves for agonist-elicited currents.

This work was supported by National Institutes of Health Grant NS23885. M.M.W. is an Established Investigator of the American Heart Association.

In the case of the muscle-type AChR, two groups have examined the effects of phenylalanine substitution at positions αY190 (αY190F mutation) and αY198 (αY198F), in AChRs from mouse muscle (5) and *Torpedo* electroplax (6), on the functional properties of receptors. Both groups observed essentially the same shifts in the dose-response curves but arrived at very different conclusions concerning the underlying cause of the shift. Tomaselli *et al.* (5) concluded that the mutations decreased the true binding affinity for ACh, whereas O'Leary and White (6) concluded that the mutations altered the coupling of ligand binding to channel opening, with little effect on agonist affinity. However, both groups based their conclusions on rather indirect experimental approaches, i.e., binding experiments under conditions where most of the receptors should be in the desensitized, not activatable, state in the case of the mouse AChR and analysis of the effects of the mutations on the actions of partial agonists in the activation of wild-type and mutant receptors in the case of the *Torpedo* receptor. Neither approach can directly determine the mechanism that underlies the alteration of the properties of the resting activatable state of the receptor.

In this report, we have used the kinetic analysis of the gating of wild-type, αY93F, and αY198F mouse muscle AChRs at the single-channel level to obtain estimates for the rate constants involved in both the agonist binding/unbinding reactions and the channel opening/closing reactions. We find that the main

ABBREVIATIONS: AChR, acetylcholine receptor; ACh, acetylcholine; PTMA, phenyltrimethylammonium; HEPES, 4-(2-hydroxyethyl)-1-piperazineethanesulfonic acid; EGTA, ethylene glycol bis(β-aminoethyl ether)-*N*,*N*,*N*′,*N*′-tetraacetic acid.

effect of the mutations is to decrease the affinity of ACh for the receptor, with little effect on the coupling of ligand binding to channel opening. A surprising result of this analysis is that the underlying cause of the decrease in agonist affinity is not an increase in the agonist dissociation rate but, rather, a decrease in the agonist association rate.

Materials and Methods

Plasmids and site-directed mutagenesis. Mouse muscle AChR subunit cDNAs were obtained from Dr. J. P. Merlie (Washington University) (α subunit), N. Davidson (California Institute of Technology) (β and δ subunits), and S. Heinemann (Salk Institute) (γ subunit). The α subunit was subcloned into the pALTER-1 vector (Promega, Madison, WI).

Mutagenesis of the α subunit was carried out using the commercially available Altered Sites system (Promega). The mutagenic primers were 17–21 nucleotides in length and were synthesized using an Applied Biosystems model 391 oligonucleotide synthesizer. Mutations were confirmed by sequence analysis through the entire coding region, using the Sanger dideoxy termination method (Sequenase; United States Biochemicals, Cleveland, OH), to verify that only the desired nucleotide changes were present.

***In vitro* transcription and expression in *Xenopus* oocytes.** Plasmid DNAs were linearized with the appropriate restriction enzymes and transcribed *in vitro* using SP6 RNA polymerase, as described previously (7). Oocytes were harvested from mature female *Xenopus laevis* (Xenopus One, Ann Arbor, MI) and the adhering follicle cell layer was removed using collagenase (type IA; Sigma). Isolated, follicle-free oocytes were maintained in SOS (100 mM NaCl, 2 mM KCl, 1.8 mM $CaCl_2$, 1 mM $MgCl_2$, 5 mM HEPES, pH 7.6) supplemented with 2.5 mM sodium pyruvate and 50 μg/ml gentamicin. AChR subunit RNAs were mixed in a molar stoichiometry of 2:1:1:1 ($\alpha/\beta/\gamma/\delta$) and 8–15 ng were injected into the oocyte cytoplasm. Oocytes were maintained in SOS supplemented with pyruvate and gentamicin at 19° for 18–72 hr before recording.

Electrophysiology. Currents elicited by bath application of various concentrations of ACh were measured using a standard two-microelectrode voltage clamp [either GeneClamp 500 (Axon Instruments, Foster City, CA) or OC-725 (Warner Instruments, Hamden, CT)], at a holding potential of −70 mV. Electrodes were filled with 3 M KCl and had resistances of 0.5–3 MΩ. The recording chamber was continuously perfused with a low-Ca^{2+} saline solution (100 mM NaCl, 2 mM KCl, 0.1 mM $CaCl_2$, 5 mM $MgCl_2$, 10 mM HEPES, pH 7.6) containing 0.3 μM atropine to block any residual muscarinic AChRs that remained after removal of the follicle cells. The low-Ca^{2+} saline solution was used to reduce receptor desensitization, which is enhanced by external Ca^{2+} (8, 9).

Single-channel currents were recorded in the outside-out mode (10) using an Axopatch 1B amplifier to avoid contributions from endogenous stretch-activated channels (11). Pipettes were filled with 80 mM KF, 20 mM KCl, 10 mM EGTA, 10 mM HEPES, pH 7.4, and had resistances between 7 and 20 MΩ. Excised patches were continually perfused with a solution containing 100 mM KCl, 10 mM EGTA, and 10 mM HEPES, pH 7.4, with the desired concentration of ACh, and were held at a potential of −100 mV. The high K^+ concentration increased the single-channel conductance from 60 to 75 pS, increasing the signal to noise ratio. Single-channel currents were filtered at 4–10 kHz (−3-db frequency, eight-pole Bessel filter) and digitized at 47 kHz (VR-10B digitizer; Instrutech, Elmont, NY) before storage on tape. Covarrubias and Steinbach (12) have reported that excised patches show a 3-fold decrease in the mean open time, compared with cell-attached patches, and that this modification takes >5–10 min. Therefore, to reduce kinetic variability, data were recorded from patches 8–15 min after excision.

ACh blocks AChR channels in a voltage-dependent fashion, with a zero-voltage dissociation constant on the order of 20 mM (13). Such a block would lead to a reduction in the amplitude of macroscopic and single-channel currents at high ACh concentrations and negative membrane potentials. At −100 mV this block does not become significant until the ACh concentration exceeds 1 mM; therefore, in this study, ACh concentrations were limited to ≤1 mM.

Data analysis. Macroscopic dose-response curves from individual oocytes were fit to eq. 1a by using a Levenberg-Marquardt algorithm in a commercially available software package (Igor; WaveMetrics, Oswego, OR).

$$I = \frac{I_{max}}{1 + (EC_{50}/[A])^n} \quad (1a)$$

I and I_{max} are the currents at a given ACh concentration [A] and the maximal value, respectively, EC_{50} is the concentration of ACh required to obtain half-maximal current, and n is the apparent Hill coefficient. Data from individual oocytes were normalized to the value of I_{max} determined for that oocyte, and then the normalized data from three to seven oocytes were fit to eq. 1b to obtain final estimates of EC_{50} and n:

$$\theta = [1 + (EC_{50}/[A])^n]^{-1} \quad (1b)$$

where θ is the normalized current (I/I_{max}).

Single-channel data were transferred from tape to an Atari computer at a 47-kHz sampling rate, using a digital interface (IT-16; Instrutech). Single-channel transitions were detected using a half-amplitude detection algorithm (TAC; Instrutech). Open- and closed-time histograms were binned and displayed using a square-root ordinate and a logarithmic time axis (14). Data in the form of event tables that contained the absolute time of occurrence, amplitude, dwell time, and type of transition (opening or closing) were then transferred to a 80486-based computer, where the rest of the analysis was carried out.

At high agonist concentrations, channel activity appears as clusters of openings separated by long quiet periods corresponding to desensitized states (15). Closed-time histograms at high agonist concentrations have predominant short duration components and minor long duration components that correspond to channel closures and desensitization, respectively. A limit closed time was selected as the time at which the two classes of components intersect, which minimizes the total number of misclassifications (16). The table of events was divided into clusters of activity using the limit closed time; in other words, any closing that lasted longer than the limit closed time was considered to be the end of the cluster. Rate constants for the different steps in the opening process were estimated from the data by the maximum-likelihood method (17), using a fitting routine provided by Dr. Richard Horn (Thomas Jefferson University) that contains an algorithm that corrects for missed events caused by the limited bandwidth of the recording conditions. Errors were estimated using the technique of resampling with replacement (18). Each patch was resampled five to eight times to obtain estimates of the errors associated with each individual rate constant in a given patch. The values from three patches for each receptor were then used to obtain the values given in Table 3.

Results

Tyrosines at positions 93, 190, and 198 (αY93, αY190, and αY198) are found in all AChR α subunits cloned to date. Mutagenesis studies on neuronal (αY93 and αY190) (19), mouse muscle (αY190 and αY198) (5), and *Torpedo* (αY190 and αY198) (6) AChRs employing phenylalanine for tyrosine substitutions have suggested that these residues play an important role in ligand-induced channel opening. We have made all three substitutions (αY93F, αY190F, and αY198F) in a single receptor type, the mouse muscle AChR, to analyze the effects of these mutations in both a qualitative and quantitative fashion. Fig. 1 and Table 1 show the effects of these three mutations on the macroscopic dose-response relationship for ACh. In all

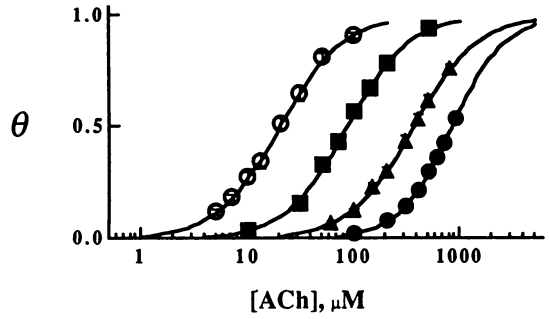

Fig. 1. Dose-response curves for AChRs with phenylalanine for tyrosine substitutions. Oocytes expressing either wild-type or mutant AChRs were voltage clamped at −70 mV, and the currents elicited by bath application of various concentrations of ACh were measured. Currents from individual oocytes were normalized as described in the text. Each *point* represents the mean ± standard error of five to seven determinations. The *smooth curves* are described by eq. 1b, using the parameters listed in Table 1. ○, Wild-type; ▲, αY93F; ●, αY190F; ■, αY198F.

TABLE 1

Comparison of macroscopic ACh dose-response data for wild-type and mutant receptors

Concentrations of ACh required for half-maximal current (EC_{50}) and the apparent Hill coefficients (n) were estimated from fits of dose-response data to eq. 1b, as described in the text. Each value is the mean ± standard error of five to seven determinations.

Receptor	EC_{50}	n
	μM	
Wild-type	19.3 ± 0.6	1.5 ± 0.1
αY93F	353.2 ± 16.4	1.4 ± 0.1
αY190F	812.3 ± 36.0	1.7 ± 0.1
αY198F	88.1 ± 2.9	1.5 ± 0.1

three cases, substitution of phenylalanine for tyrosine led to a shift in the dose-response relationship towards higher concentrations, with no effect on the apparent Hill coefficient. Wild-type receptors were half-maximally activated at 20 μM ACh, whereas the mutant receptors were half-maximally activated at 350 μM (αY93F), 810 μM (αY190F), and 90 μM (αY198F) ACh. This decrease in the apparent affinity of ACh for the mutant receptors has been ascribed to a decrease in either agonist affinity (5) or coupling of agonist binding to channel opening (6).

Macroscopic current measurements such as these cannot allow one to distinguish between these two possibilities, because a decrease in either agonist affinity or the coupling of ligand binding to channel opening can lead to a rightward shift in the macroscopic dose-response curve (6). Ligand-binding techniques can, in principle, determine the true affinity of an agonist for its binding site, but in the case of the AChR the presence of the high affinity desensitized state means that any equilibrium binding assay will determine the affinity of this absorbing high affinity state, rather than the resting activatable state of the receptor (20–22). Initial-rate agonist/α-^{125}I-bungarotoxin competition assays have been used with cultured cells to obtain a lower limit for the affinity of the receptor in its resting state (23); however, the low density of receptors on the oocyte surface and the rapid time scale in which these measurements must be made makes these initial rate measurements unfeasible with intact oocytes, where the measurements should be made for correlation of binding data with the functional studies.

An alternate approach is to determine the rate constants of each step in the gating process, using high-resolution single-channel recording. In this approach, analysis of the dwell times of the receptor in both the closed and open states, in terms of a kinetic model, allows one to obtain estimates of the rate constants for each transition in the process (24, 25). Therefore, we carried out single-channel analysis of wild-type, αY93F, αY190F, and αY198F receptors in excised outside-out patches. Three different ACh concentrations, which spanned the range of receptor activation in the macroscopic dose-response curves for the receptors, were used.

Initial perfusion of excised patches with various concentrations of ACh frequently elicited multiple conductance levels, indicating the presence of more than one channel in the patch. However, the slow perfusion rate made determination of the exact number of channels in the patch impossible. Fig. 2 shows representative recordings of single-channel activity from an excised patch containing wild-type receptors recorded at low (1 μM), intermediate (20 μM), and high (100 μM) agonist concentrations. At low agonist concentration, channel openings appeared at a low frequency; however, because more than one channel was usually present in a patch, it was not possible to associate the closed times to the gating of a single receptor molecule. At intermediate concentrations, channel activity was increased but the same ambiguity with respect to closed times was present. Therefore, the only useful information obtained under either of these conditions was the mean open time, which is the reciprocal of the closing rate constant, α. Table 2 shows the mean open times for each receptor at low concentration.

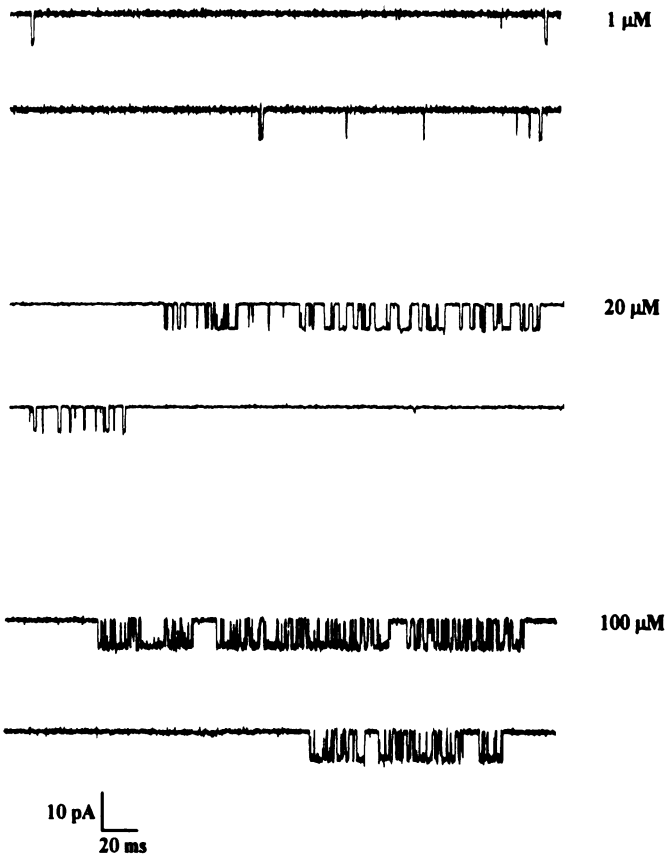

Fig. 2. Single-channel activity of wild-type AChRs. Single channels were recorded from outside-out excised patches exposed to the indicated concentrations of ACh. Note the appearance of clusters at high (100 μM), but not low (1 μM), concentrations.

TABLE 2

Mean open times for wild-type and mutant AChRs

Single-channel currents were recorded from excised patches exposed to 100 (wild-type, αY93F, and αY198F) or 400 μM (αY190F) ACh, and then mean open times were determined. The values for the mutant receptors are significantly different from those for the wild-type receptor ($p < 0.02$).

Receptor	Mean open time
	msec
Wild-type	1.80 ± 0.02
αY93F	0.92 ± 0.02
αY190F	1.10 ± 0.06
αY198F	1.28 ± 0.02

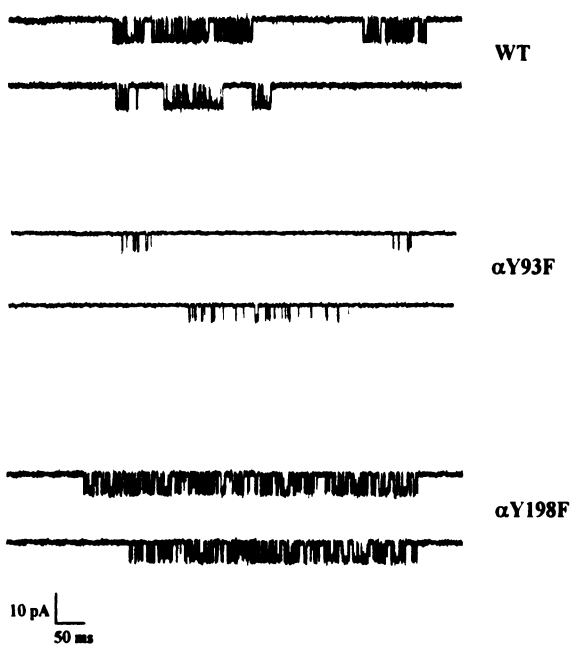

Fig. 3. Clusters of channel openings at high agonist concentrations. Single channels were recorded from excised outside-out patches from oocytes expressing the indicated receptor, with either 100 μM [wild-type (*WT*)] or 400 μM (αY93F and αY198F) ACh.

Subconductance states were infrequent (<10% of the openings in those few patches where they were observed), in agreement with most (26, 27) but not all (28) reports of AChRs expressed in *Xenopus* oocytes. Our analysis focused only on the major conductance state of the channel.

At high agonist concentrations, clusters of channel activity separated by quiet periods were observed. Fig. 3 shows representative traces of single-channel activity at high concentrations for wild-type, αY93F, and αY198F receptors, which show groups of openings separated by long quiet periods. Under these conditions, transitions within a group or cluster can be associated with the gating of a single receptor complex (15). Within a cluster one channel moves among all of the activatable states, and between clusters all channels in the patch are in the desensitized state. αY190F receptors did not show well defined clusters, even at 1 mM ACh, which is consistent with previous studies with mouse and *Torpedo* αY190F receptors, which showed that αY190F receptors desensitized very slowly (5, 6).

Estimates of the rate constants for the gating process were obtained from analysis of transitions within bursts for wild-type, αY93F, and αY198F receptors; αY190F receptors were not be analyzed further due to the lack of well defined clusters. Data were analyzed in terms of the consensus minimal model for receptor gating, in which two agonist molecules must bind to the receptor before channel opening (29, 30):

$$A + R \underset{k_{-1}}{\overset{k_{+1}}{\rightleftarrows}} A + AR \underset{k_{-2}}{\overset{k_{+2}}{\rightleftarrows}} A_2R \underset{\alpha}{\overset{\beta}{\rightleftarrows}} A_2R^*$$

where A is the agonist, R is the unoccupied receptor, AR and A_2R are the monoliganded and biliganded closed-channel forms of the receptor, respectively, and A_2R^* is the biliganded open-channel form of the receptor. The rate constants k_{+1}, k_{-1}, k_{+2}, and k_{-2} are associated with agonist binding and unbinding, whereas β and α are associated with the actual opening and closing of the channel. The desensitized states of the receptor, which are beyond the A_2R^* state, are not shown here and are not part of the analysis because they do not exist within a cluster.

The consensus minimal model predicts that the channel open-time distribution should be described by a single-exponential function and that the time constant for this distribution should be the reciprocal of the channel closing rate constant α. In addition, the closed-time distribution should show multiple exponential components. Fig. 4 shows the open- and closed-time distributions of channels recorded from αY93F receptors at high ACh concentration. The open-time distribution is well fit by a single-exponential function with a time constant of 1.0 msec, whereas the closed-time distribution is described by three exponential components with time constants of 5.5, 18, and 1300 msec, of which the two shorter durations are the closings within a cluster (the longer duration corresponds to the desensitized state). Similar behavior was seen for wild-type and aY198F receptors (data not shown). At a given ACh concentration, the closed-time distributions for the mutant receptors were shifted to longer times than that of the wild-type receptor (data not shown).

The rate constants for each of the steps in the activation process were estimated using the maximum-likelihood method (17). In this method, the likelihood of observing the experimental data given a specific kinetic model and set of rate constants is estimated, and then the rate constants are varied until the likelihood is at a maximum [or −log(likelihood) is at a minimum]. For each fit, the closing rate constant α was constrained to be the reciprocal of the value obtained from the single-exponential fit of the open-time distribution for that particular patch. Table 3 shows the estimates for the rate constants

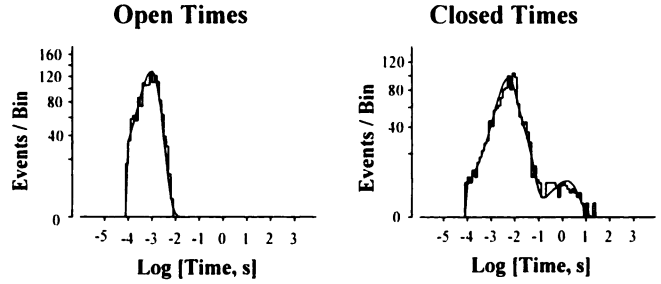

Fig. 4. Open- and closed-time distributions for αY93F receptors. Single-channel openings were recorded from excised patches exposed to 1 mM ACh, and the open and closed times were binned and displayed as described in Materials and Methods. The *smooth curve in the open-time distribution* represents a fit of the distribution to a single-exponential function with a time constant of 1.0 msec, whereas the *smooth curve in the closed-time distribution* represents the sum of three exponential components with time constants of 5.5, 18, and 1300 msec and relative areas of 65%, 30%, and 5%, respectively.

TABLE 3

Rate constants derived from single-channel data

Rate constants for the steps in the four-state kinetic model presented in the text were estimated using the maximum-likelihood method. Values are presented as mean ± standard error from three patches for each receptor. The dissociation constants for the two binding sites, K_1 and K_2, were calculated from the association and dissociation rates for the two binding steps.

Receptor	k_{+1}	k_{-1}	k_{+2}	k_{-2}	β	α	K_1	K_2	β/α
	M^{-1} sec^{-1}	sec^{-1}	M^{-1} sec^{-1}	sec^{-1}	sec^{-1}	sec^{-1}	μM	μM	
Wild-type	4.5 ± 0.9 × 10^6	304 ± 73	5.5 ± 0.6 × 10^7	10,174 ± 783	8,777 ± 377	886 ± 45	68 ± 21	185 ± 25	9.9 ± 0.7
αY93F	8.1 ± 1.7 × 10^{5*}	348 ± 84	3.1 ± 0.3 × 10^{5*}	14,815 ± 1,200*	11,165 ± 215*	1,569 ± 38*	429 ± 137*	47,790 ± 6,030*	7.1 ± 0.2*
αY198F	4.1 ± 0.5 × 10^6	747 ± 83*	5.7 ± 0.6 × 10^{6*}	9,825 ± 1,006	9,537 ± 263	1,047 ± 44*	182 ± 30*	1,723 ± 253*	9.1 ± 0.5

* Statistically different from the wild-type value ($p < 0.02$).

obtained using this procedure with data collected from three different patches for each receptor at high ACh concentrations (100 μM for the wild-type receptor, 1 mM for the αY93F receptor, and 400 μM for the αY198F receptor), as well as the calculated binding constants for the two binding steps, K_1 and K_2, and the equilibrium constant for channel opening, β/α. It can be seen that neither mutation has a major effect on the channel opening equilibrium constant (β/α), indicating that the coupling process is relatively unaffected. However, the binding rate constants for the two mutations are affected. In the case of αY93F receptors, both association rate constants (k_{+1} and k_{+2}) decrease, along with a 50% increase in the dissociation rate for the second binding step, k_{-2}, leading to a reduction in the affinity of both sites for ACh. In the case of αY198F receptors, k_{-1} is doubled and k_{+2} is decreased, which leads to a reduction of affinity of both binding sites.

Discussion

A growing body of evidence suggests that amino acids αY93, αY190, and αY198 form at least a portion of the ligand binding site of AChRs. In particular, replacement of these tyrosines by phenylalanine in *Torpedo* (6, 31), mouse muscle (5), or α7 neuronal (19) receptors leads to a shift in the midpoints of the dose-response curves for agonist-evoked currents toward higher concentrations. The midpoint of the dose-response curve (EC_{50}) is a purely empirical parameter that depends upon the rate constants for ligand binding and unbinding, as well as those for channel opening and closing. Therefore, changes in either agonist affinity or the coupling of binding to channel opening could alter EC_{50}, and one cannot unequivocally determine the underlying cause of the shift solely from measurements of currents evoked by ACh. The shift observed after mutation has been ascribed to a decrease in either agonist affinity (5) or coupling of ligand binding to channel opening (6). In the former case Tomaselli *et al.* (5) based their conclusion on the fact that the IC_{50} for inhibition by ACh of the binding of the competitive antagonist α-bungarotoxin under quasi-equilibrium conditions (where the bulk of the receptors should be in the desensitized state, which is known to have an affinity different from that of the resting state of the receptor) (20–22) was shifted in a similar fashion as were the EC_{50} values for channel opening, whereas in the latter case O'Leary and White (6) based their conclusion on the fact that the mutations converted the partial agonists PTMA and tetramethylammonium into competitive antagonists with IC_{50} values similar to their EC_{50} values for activation of wild-type receptors. Both approaches suffer from the fact that they are both rather indirect methods for assessing changes in the affinity of the receptor in the resting activatable state.

We have tried to address this question directly by obtaining estimates for all of the rate constants in the gating scheme using the analysis of single-channel kinetics. The analysis of channel gating kinetics using single-channel recordings is a computationally intensive process that depends upon the model(s) used, and therefore one's intuition may be of little use in evaluating the results of the extensive fitting involved. As with any such process, it is important to be able to separate the model-dependent from the model-independent (or nearly model-independent) conclusions. In the case of the data presented here, the fact that the mean open time does not change much with the tyrosine to phenylalanine substitutions (<2-fold at most) (Table 2) strongly suggests that the conformational change associated with channel closing is relatively unaffected by the mutations. A reasonable extension of this finding would be to hypothesize that the reverse conformational change, the actual channel opening itself, is also relatively unaffected by the mutations. A second model-independent conclusion is that the mean closed times for the mutant receptors are greater than those for the wild-type receptors at a given ACh concentration. Given the previous conclusion/hypothesis that the opening rate is relatively unaffected by the mutations, this suggests that an earlier event (or events) in the process, involving ligand binding, is slower.

Given these model-independent (or nearly model-independent) conclusions concerning the effects of the mutations on AChR gating, we can then use the maximum-likelihood method in conjunction with the consensus minimal model for receptor gating to localize the particular transitions affected by the mutations. As expected/hypothesized from the model-independent analysis of channel open- and closed-time distributions, the overall conclusion from the single-channel analysis is that the predominant effect of the αY93F and αY198F mutations is to alter the affinity of the agonist binding sites, rather than the coupling of binding to opening. In addition, in the case of the αY93F receptor there is a small, albeit statistically significant, decrease in coupling of ligand binding to channel opening, but this is a relatively minor effect. Thus, at least in the case of the αY198F mutation (which was studied by both groups), the conclusion of Tomaselli *et al.* concerning the underlying mechanism is correct and that of O'Leary and White is incorrect. Although the two groups used AChRs from different species, we consider it unlikely that the same mutation in a highly conserved subunit could have different mechanistic effects on AChRs in two different species; rather, this points to the shortcomings of indirect approaches. For example, the currents evoked by PTMA and tetramethylammonium from wild-type *Torpedo* AChRs are small, compared with those evoked by ACh, and it is possible that those evoked by the partial agonists from the mutant AChRs were too small to

detect. In support of this notion, we have been able to measure small PTMA-evoked currents from αY93F, αY190F, and αY198F mutant mouse AChRs (32). This is most likely due to the fact that macroscopic currents recorded from mouse AChRs expressed in oocytes are much larger and desensitize more slowly than their *Torpedo* counterparts at a given ACh concentration, allowing the detection of much smaller fractional currents. In addition, the fact that in the *Torpedo* AChR changes in the affinity of the competitve antagonist curare (αY93F and αY190F receptors) and the apparent affinity of the partial agonist PTMA (αY93F and αY198F receptors) are similar to changes in the EC_{50} for ACh (31, 32) suggests that these residues are involved in ligand-receptor interactions.

To compare the effects of the mutations on the single-channel kinetics and the observed shifts in the macroscopic dose-response curves, theoretical dose-response curves were calculated using the rate constants obtained from the maximum-likelihood analysis for wild-type, αY93F, and αY198F receptors. Fig. 5 shows the macroscopic data redrawn from Fig. 1 and the calculated curve for wild-type receptors. At first glance the agreement appears poor; however, there are two factors that could cause the macroscopic dose-response curves to be shifted to the left, relative to those calculated from the single-channel kinetic data. First, receptor desensitization and open-channel block could cause the macroscopic dose-response curve to be shifted to the left, relative to that obtained from single-channel recordings (33). Second, the single-channel data were obtained from excised patches, whereas the macroscopic data were obtained from intact oocytes. Covarrubias and Steinbach (12) have shown that excision of patches from mouse BC_3H_1 cells leads to an alteration in the single-channel gating properties of AChRs. In particular, α increases by about 3-fold and β/k_{-2} decreases to half its value in cell-attached patches. The net effect of these changes would be to shift the dose-response curve to the right in the excised patches, relative to the cell-attached patches. Evidence that this phenomenon also occurs in oocytes comes from the fact that Auerbach (34) reported values of α for wild-type BC_3H_1 AChRs expressed in *Xenopus* oocytes in cell-attached patches at −100 mV (the voltage used in our experiments) to be on the order of 300 sec^{-1}, approximately one third of the value that we observe in excised patches for the same receptors.

Table 4 compares the EC_{50} values from the macroscopic current experiments with those obtained from fitting the theoretical dose-response curves to eq. 1b. As is the case for the wild-type receptors, the midpoints of the theoretical curves for the mutants are 3–6 times higher than those of the macroscopic curves. However, the shifts in the curves for the mutants, relative to the wild-type receptors, are similar for both sets of curves. When the ratios of the EC_{50} values are used to compute the apparent free energy difference of the mutants, relative to the wild-type receptors, for both the macroscopic and deduced single-channel curves, the two sets of data give similar changes. Therefore, although the absolute positions of the two sets of curves are different, the two sets show the same relative effect, suggesting that the underlying cause is the same.

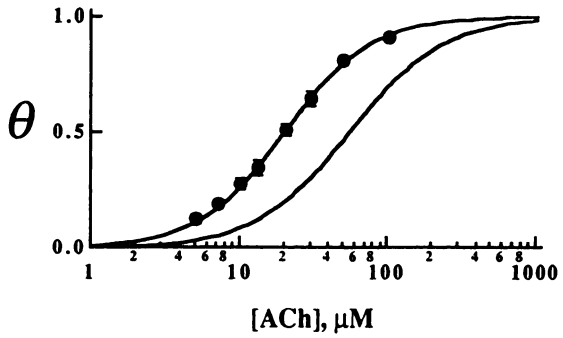

Fig. 5. Comparison of macroscopic and deduced microscopic dose-response curves for wild-type AChRs. The theoretical dose-response curve constructed using the parameters obtained from the single-channel analysis, as described in the legend to Table 4 (*right curve*), is shown along with the macroscopic dose-response curve for wild-type receptors redrawn from Fig. 1 (*left curve*).

TABLE 4

Comparison of macroscopic and single-channel fits

Macroscopic EC_{50} values for ACh are from Table 1. Single-channel EC_{50} values were obtained by generating curves describing the concentration dependence of the probability of opening, using the rate constants derived from the maximum-likelihood analysis, with the following relation (40):

$$p_{open} = \frac{c_1c_2\left(\frac{\beta}{\alpha}\right)}{1 + 2c_1 + c_1c_2\left[1 + \left(\frac{\beta}{\alpha}\right)\right]}$$

where $c_1 = \frac{k_{+1}[ACh]}{k_{-1}}$ and $c_2 = \frac{kei+2[ACh]}{k_{-2}}$. Thus curve was then fit to eq. 1a to obtain EC_{50} values. The change in free energy due to the mutation, Δ(ΔG), is defined as

$$\Delta(\Delta G) = RT\ln\frac{EC_{50}\text{ (mut)}}{EC_{50}\text{ (WT)}}$$

where EC_{50} (mut) and EC_{50} (WT) are the EC_{50} values for the mutant and wild-type receptors, respectively.

Receptor	Macroscopic		Single-channel	
	EC_{50}	Δ(ΔG)	EC_{50}	Δ(ΔG)
	μM	kcal/mol	μM	kcal/mol
Wild-type	19.3		53.6	
αY93F	352	1.7	2140	2.1
αY198F	88	0.9	350	1.1

The main effect of the αY93F and αY198F mutations appears to be on the forward rate constants for ACh binding, especially on k_{+2}. At first glance this seems anti-intuitive, because one might assume that alterations in the off-rate would be the underlying cause of a change in the dissociation constant. However, based on electron image reconstruction at 9-Å resolution, Unwin (35) has proposed that the ACh binding sites on the AChR have a narrow cleft that ACh must traverse as it binds to the receptor, similar to the "aromatic gorge" in the binding site of acetylcholinesterase (36). If this is the case and αY93 and αY198 either are in this cleft or interact with residues that form it, then one can conceive of a situation where a mutation could decrease the on-rate of ACh by changing the "landscape" of the cleft, making it more difficult for ACh to enter. If the conformation of the binding site with the agonist bound is different from that in the unliganded receptor (as expected for an allosteric model of gating) (37, 38) and/or ACh leaves the binding site by a different pathway than that by which it enters, then this could explain why the association rate but not the dissociation rate is affected.

While this manuscript was in preparation, an abstract appeared presenting results similar to those presented here. Zhang *et al.* (39) examined the single-channel gating kinetics of wild-type, αY93F, and αY198F mouse AChRs. Based on their preliminary results, those authors concluded that the main effect

of the mutations was to decrease the agonist association rate, just as we found.

The overall conclusion of this work is that mutations in the putative binding domain behave as others have concluded, i.e., they alter the affinity of the binding site for ACh (5, 19). However, it is important to point out that those conclusions were based on indirect measurements. Although our results are in agreement with these other studies, they were obtained using detailed analysis of single-channel gating, which allows one to directly address the question of the underlying mechanism of the shifts in the macroscopic dose-response curves. In particular, we are able to determine whether a mutation affects the agonist association rate or the dissociation rate, a distinction that cannot be easily made using conventional ligand binding assays. Additional investigations using a wider variety of substitutions at positions αY93, αY190, and αY198, as well as extended adjacent areas, should allow us to further define agonist-receptor interactions and thus gain insight into how the AChR (as well as other members of the ligand-gated ion channel family) couples agonist binding to channel opening.

Acknowledgments

We would like to thank Dr. R. Horn for the maximum-likelihood analysis programs and Drs. S. Garber, R. Preston, and J. Russell for their helpful comments.

References

1. Betz, H. Homology and analogy in transmembrane channel design: lessons from synaptic membrane proteins. *Biochemistry* **29**:3591–3599 (1990).
2. Stroud, R. M., M. P. McCarthy, and M. Shuster. Nicotinic acetylcholine receptor superfamily of ligand-gated ion channels. *Biochemistry* **29**:11009–11023 (1990).
3. Karlin, A. Structure of nicotinic acetylcholine receptors. *Curr. Opin. Neurobiol.* **3**:299–309 (1993).
4. Devillers-Thiery, A., J. L. Galzi, J. L. Eisele, S. Bertrand, D. Bertrand, and J. P. Changeux. Functional architecture of the nicotinic acetylcholine receptor: a prototype of ligand-gated ion channels. *J. Membr. Biol.* **136**:97–112 (1993).
5. Tomaselli, G. F., J. T. McLaughlin, M. E. Jurman, E. Hawrot, and G. Yellen. Mutations affecting agonist sensitivity of the nicotinic acetylcholine receptor. *Biophys. J.* **60**:721–727 (1991).
6. O'Leary, M. E., and M. M. White. Mutational analysis of ligand-induced activation of the *Torpedo* acetylcholine receptor. *J. Biol. Chem.* **267**:8360–8365 (1992).
7. Buller, A. L., and M. M. White. Control of *Torpedo* acetylcholine receptor biosynthesis in *Xenopus* oocytes. *Proc. Natl. Acad. Sci. USA* **85**:8717–8721 (1988).
8. Manthey, A. A. The effect of calcium on the desensitization of membrane receptors at the neuromuscular junction. *J. Gen. Physiol.* **49**:963–976 (1966).
9. Miledi, R. Intracellular calcium and the desensitization of acetylcholine receptors. *Proc. R. Soc. Lond. B. Biol. Sci.* **209**:447–452 (1980).
10. Hamill, O. P., A. Marty, E. Neher, B. Sakmann, and F. J. Sigworth. Improved patch-clamp techniques for high-resolution recording from cells and cell-free membrane patches. *Pfluegers Arch.* **391**:85–100 (1981).
11. Methfessel, C., V. Witzmann, T. Takahashi, S. Numa, and B. Sakmann. Patch clamp measurements on *Xenopus laevis* oocytes: currents through endogenous channels and implanted acetylcholine receptor and sodium channels. *Pfluegers Arch.* **407**:577–588 (1986).
12. Covarrubias, M., and J. H. Steinbach. Excision of membrane patches reduces the mean open time of nicotinic acetylcholine receptors. *Pfluegers Arch.* **416**:385–392 (1990).
13. Sine, S. M., and J. H. Steinbach. Agonists block currents through acetylcholine receptor channels. *Biophys. J.* **46**:277–284 (1984).
14. Sigworth, F. J., and S. M. Sine. Data transformations for improved display and fitting of single-channel dwell time histograms. *Biophys. J.* **52**:1047–1054 (1987).
15. Sakmann, B., J. Patlak, and E. Neher. Single acetylcholine-activated channels show burst-kinetics in the presence of desensitizing concentrations of agonist. *Nature (Lond.)* **286**:71–73 (1980).
16. Jackson, M. B., B. S. Wong, C. E. Morris, H. Lecar, and C. N. Christian. Successive openings of the same acetylcholine receptor are correlated in open time. *Biophys. J.* **42**:109–114 (1983).
17. Horn, R., and K. Lange. Estimating kinetic constants from single-channel data. *Biophys. J.* **43**:207–233 (1983).
18. Horn, R. Statistical methods for model discrimination: applications to gating kinetics and permeation of the acetylcholine receptor chanel. *Biophys. J.* **51**:255–263 (1987).
19. Galzi, J.-L., D. Bertrand, A. Devillers-Thiery, F. Revah, S. Bertrand, and J.-P. Changeux. Functional significance of aromatic amino acids from three peptide loops of the α7 neuronal nicotinic receptor site investigated by site-directed mutagenesis. *FEBS Lett.* **294**:198–202 (1991).
20. Weber, M., T. David-Pfeuty, and J.-P. Changeux. Regulation of the binding properties of the nicotinic receptor protein by cholinergic ligands in membrane fragments from *Torpedo marmorata*. *Proc. Natl. Acad. Sci. USA* **72**:3443–3447 (1975).
21. Weiland, G., B. Georgia, V. T. Wee, C. F. Chignell, and P. Taylor. Ligand interactions with cholinergic receptor-enriched membranes from *Torpedo*: influence of agonist exposure on receptor properties. *Mol. Pharmacol.* **12**:1091–1105 (1976).
22. Weiland, G., B. Georgia, S. Lappi, C. F. Chignell, and P. Taylor. Kinetics of agonist-mediated transitions in the state of the cholinergic receptor. *J. Biol. Chem.* **252**:7648–7656 (1977).
23. Sine, S., and P. Taylor. Functional consequences of agonist-induced state transitions in the cholinergic receptor: studies in cultured muscle cells. *J. Biol. Chem.* **254**:3315–3325 (1979).
24. Colquhoun, D., and A. G. Hawkes. On the stochastic properties of single ion channels. *Proc. R. Soc. Lond. B. Biol. Sci.* **211**:205–235 (1981).
25. Colquhoun, D., and A. G. Hawkes. On the stochastic properties of bursts of single ion channel openings and of clusters of bursts. *Philos. Trans. R. Soc. Lond. B Biol. Sci.* **300**:1–59 (1982).
26. Sakmann, B., C. Methfessel, M. Mishina, T. Takahashi, M. Takai, K. Kurasaki, K. Fukuda, and S. Numa. Role of acetylcholine receptor subunits in gating of the channel. *Nature (Lond.)* **318**:538–543 (1985).
27. Yu, L., R. J. Leonard, N. Davidson, and H. A. Lester. Single-channel properties of mouse-*Torpedo* acetylcholine receptor hybrids expressed in *Xenopus* oocytes. *Mol. Brain Res.* **10**:203–211 (1991).
28. Kullberg, R., J. L. Owens, P. Camacho, G. Mandel, and P. Brehm. Multiple conductance classes of mouse nicotinic acetylcholine receptors expressed in *Xenopus* oocytes. *Proc. Natl. Acad. Sci. USA* **87**:2067–2071 (1990).
29. Adams, P. R. An analysis of the dose-response curve at voltage-clamped frog endplates. *Pfluegers Arch.* **360**:145–153 (1975).
30. Adams, P. R. Relaxation experiments using bath-applied suberyldicholine. *J. Physiol. (Lond.)* **268**:271–289 (1977).
31. O'Leary, M. E., G. N. Filatov, and M. M. White. Characterization of the *d*-tubocurarine binding site of *Torpedo* acetylcholine receptor. *Am. J. Physiol.* **266**:C648–C653 (1994).
32. Aylwin, M. A., and M. M. White. Ligand-receptor interactions in the nicotinic acetylcholine receptor probed using multiple substitutions at conserved tyrosines in the α subunit. *FEBS Lett.* **349**:99–103 (1994).
33. Lingle, C. J., D. Maconochie, and J. H. Steinbach. Activation of skeletal muscle nicotinic acetylcholine receptors. *J. Membr. Biol.* **126**:195–217 (1992).
34. Auerbach, A. Kinetic behavior of cloned mouse acetylcholine receptors: a semi-autonomous, stepwise gating model of gating. *Biophys. J.* **62**:72–73 (1992).
35. Unwin, N. Nicotinic acetylcholine receptor at 9 Å resolution. *J. Mol. Biol.* **229**:1101–1124 (1993).
36. Sussman, J. L., M. Harel, F. Frolow, C. Oefner, A. Goldman, L. Toker, and I. Silman. Atomic structure of acetylcholinesterase from *Torpedo californica*: a prototypic acetylcholine-binding protein. *Science (Washington D. C.)* **253**:872–879 (1991).
37. Monod, J., J. Wyman, and J.-P. Changeux. On the nature of allosteric transitions: a plausible model. *J. Mol. Biol.* **12**:88–118 (1965).
38. Karlin, A. On the application of "a plausible model" of allosteric proteins to the receptor for acetylcholine. *J. Theoret. Biol.* **16**:306–320 (1967).
39. Zhang, Y., J. Chen, G. Akk, S. Sine, and A. Auerbach. Single-channel kinetics of mouse AChR: mutations of α-subunit residues Y198, Y190, Y93, and D200. *Biophys. J.* **66**:A9 (1994).
40. Colquhoun, D., and D. C. Ogden. Activation of ion channels in the frog endplate by high concentrations of acetylcholine. *J. Physiol. (Lond.)* **395**:131–159 (1988).

Send reprint requests to: Michael M. White, Department of Physiology, Room 290, Medical College of Pennsylvania, 2900 Queen Lane, Philadelphia, PA 19129.